

**ANNUAL REPORTS ON
NMR SPECTROSCOPY**

Volume 29



ACADEMIC PRESS

ANNUAL REPORTS ON

NMR SPECTROSCOPY

This Page Intentionally Left Blank

ANNUAL REPORTS ON
NMR SPECTROSCOPY

Edited by

G. A. WEBB

Department of Chemistry, University of Surrey, Guildford, Surrey, England

VOLUME 29



ACADEMIC PRESS

Harcourt Brace & Company, Publishers

London • San Diego • New York
Boston • Sydney • Tokyo • Toronto

ACADEMIC PRESS LIMITED
24-28 Oval Road,
LONDON NW1 7DX

U.S. Edition Published by

ACADEMIC PRESS INC.
San Diego, CA 92101

This book is printed on acid free paper

Copyright © 1994 ACADEMIC PRESS LIMITED

All Rights Reserved

No part of this book may be reproduced or transmitted in any form or by any means, electronic or mechanical including photocopying, recording, or any information storage and retrieval system without permission in writing from the publisher

**A catalogue record for this book is available from the
British Library**

ISBN 0-12-505329-0
ISSN 0066-4103

Phototypesetting by Keyset Composition, Colchester, Essex
Printed by TJ Press Ltd, Padstow, Cornwall

List of Contributors

Tetsuo Asakura, *Department of Biotechnology, Tokyo University of Agriculture and Technology, Koganei, Tokyo 184, Japan.*

D. B. Chesnut, P. M. Gross *Chemical Laboratory, Duke University, Durham, North Carolina 27708, USA.*

I-Ssuer Chuang, *Department of Chemistry, Colorado State University, Fort Collins, Colorado 80523, USA.*

T. A. Cross, *National High Magnetic Field Laboratory, Institute of Molecular Biophysics and Department of Chemistry, Florida State University, Tallahassee, Florida 32306, USA.*

Makoto Demura, *Department of Biotechnology Tokyo University of Agriculture and Technology, Koganei, Tokyo 184, Japan.*

Angel C. de Dios, *Department of Chemistry, University of Illinois at Urbana-Champaign, 505 South Mathews Avenue, Urbana, Illinois 61801, USA.*

Tetsuo Hayashi, *Plastics Research Laboratory, Tokuyama Corp. Ltd, 1-1 Harumi-chou, Tokuyama, Yamaguchi 745, Japan.*

Cynthia J. Jameson *Department of Chemistry M/C 111, University of Illinois at Chicago, 845 W. Taylor, Chicago, Illinois 60607, USA.*

Gary E. Maciel, *Department of Chemistry, Colorado State University, Fort Collins, Colorado 80523, USA.*

Graeme Moad, *CSIRO, Division of Chemicals and Polymers, Private Bag 10, Clayton, Victoria 3168, Australia.*

This Page Intentionally Left Blank

Preface

The NMR chemical shift and the information it can provide on structure and environment is admirably reviewed by Professor C. J. Jameson and Dr A. C. DeDios in the first chapter of the present volume of *Annual Reports on NMR*. This is a welcome complement and extension of the review by Professor Jameson and Dr H. J. Osten in Volume 17 of this series. Following this is a very interesting account of *ab initio* calculations of NMR chemical shieldings, by Professor D. B. Chesnut which builds on his previous review in Volume 21 of *Annual Reports on NMR*.

The remaining four chapters cover various aspects of applications of NMR to polymers. Professor T. A. Cross reviews applications of solid state NMR to the structures of peptides and proteins in synthetic membrane environments. This is followed by an account of the NMR characterization of complex organic resins by Dr I-Ssuer Chuang and Professor G. E. Maciel. Dr G. Moad covers applications of labelling and multidimensional NMR in the characterization of synthetic polymers and the final chapter is by Professor T. Asakura, Dr M. Demura and Dr T. Hayashi who deal with ^{13}C NMR assignments of polyolefines and olefine copolymers based on ^{13}C NMR chemical shift calculations and 2D INADEQUATE data.

It is a very great pleasure for me to have the opportunity to thank all of these contributors for the preparation and timely submission of their reviews and the staff at Academic Press (London) for their help and co-operation in the production of this volume.

University of Surrey
Guildford, Surrey
England

G. A. WEBB

This Page Intentionally Left Blank

Contents

List of Contributors	v
Preface	vii

The NMR Chemical Shift: Insight into Structure and Environment **1** ANGEL C. de DIOS and CYNTHIA J. JAMESON

1. Introduction	2
2. Shielding surfaces	4
3. Dynamic averages on shielding surfaces, comparisons with experiments	29
4. Applications to more complex systems	51
5. Conclusions	63
Acknowledgement	64
References	64

***Ab Initio* Calculations of NMR Chemical Shielding** **71** D. B. CHESNUT

1. Introduction	71
2. The general problem	72
3. Basic theory	75
4. Self-consistent field approaches.	82
5. Effects of correlation	106
6. Concluding remarks	118
References	119

Structural Biology of Peptides and Proteins in Synthetic Membrane Environments by Solid-state NMR Spectroscopy **123** T. A. CROSS

1. The new frontiers in structural biology	124
2. Molecular examples	129
3. Other experimental techniques in structural biology	132
4. Solid-state NMR	135
5. Applications	144
6. Conclusions	161
Acknowledgements.	161
References	161

169

NMR Characterization of Complex Organic Resins
I-SSUER CHUANG and GARY E. MACIEL

1. Introduction	170
2. Solid-state NMR	171
3. Solid-state NMR characterization of complex organic resins	179
4. Resins in polymer blends and composite materials	271
References	274

287

**Applications of Labelling and Multidimensional NMR in the Characterization
of Synthetic Polymers**
GRAEME MOAD

1. Introduction	287
2. Chemical microstructure structure of polymer chains	288
3. Synthesis of labelled monomers	296
4. Detection and quantitation of polymer end-groups	297
5. Synthesis of labelled initiators	318
Acknowledgements	318
Abbreviations	318
References	319

325

**¹³C NMR Assignments of Polyolefines and Olefine Copolymers Based
on the ¹³C NMR Chemical Shift Calculations and
2D INADEQUATE NMR**
TETSUO ASAKURA, MAKOTO DEMURA and TETSUO HAYASHI

1. Introduction	326
2. Calculation	328
3. NMR observation	338
4. Polyolefines	339
5. Ethylene-olefine copolymers	370
6. Conclusion	401
Acknowledgements.	401
References	401

Index	405
-----------------	-----

The NMR Chemical Shift: Insight into Structure and Environment

ANGEL C. de DIOS

Department of Chemistry, University of Illinois at Urbana-Champaign, 505 South Mathews Avenue, Urbana, Illinois 61801, USA

CYNTHIA J. JAMESON

Department of Chemistry M/C 111, University of Illinois at Chicago, 845 W. Taylor, Chicago, Illinois 60607, USA

1. Introduction	2
2. Shielding surfaces	4
2.1. Intramolecular shielding surfaces	5
2.1.1. Dependence on bond length in diatomic molecules	5
2.1.2. Bond extension and angle deformation in small molecules	7
2.1.3. Dihedral angle	12
2.1.4. Remote bond extension	17
2.2. Intermolecular shielding surfaces	19
2.2.1. Distance dependence	19
2.2.2. Scaling of intermolecular shielding	21
2.2.3. Additivity and non-additivity	22
2.2.4. Hydrogen bonding	22
2.3. Electric field effects and dispersion contributions	25
2.4. Is there a global shape for the traces on shielding surfaces?	27
3. Dynamic averages on shielding surfaces, comparisons with experiments	29
3.1. The temperature dependence of the shielding in a molecule	30
3.2. Isotope effects	34
3.3. Intermolecular shifts	39
3.3.1. The chemical shift in the gas phase	40
3.3.2. The average chemical shifts of Xe in zeolites	42
3.3.2. Gas-to-liquid and gas-to-solution shifts	47
4. Applications to more complex systems	51
4.1. Separation of short-range and long-range effects on shielding	51
4.2. Use of scaling and additivity	54
4.3. Use of electric field effects and dynamic averaging	58
4.4. Predicting shifts in complex systems from shielding surfaces of model systems	60
5. Conclusions	63
Acknowledgement	64
References	64

1. INTRODUCTION

The NMR chemical shift is well known to be extremely sensitive to the environment of the nucleus. The chemical shift of a methyl proton is in a region of the proton shift that is well separated from the chemical shift of a proton in a CH_2 group, for example. Furthermore, the two protons in a CH_2 group could have distinct chemical shifts depending on the immediate neighbouring atoms of each proton. The ease of discrimination between *cis* and *trans*, *syn* and *anti* even under the lower resolution of the early spectrometers, was well known. With present-day instrumentation even subtle differences are easily observed. The NMR chemical shift discriminates between S and R enantiomers in a chiral solvent and between the various alanine residues in the same protein molecule, for example. There is no other property that has this degree of sensitivity to the electronic environment. In condensed phases there are gas-to-liquid shifts or solvent shifts, matrix-induced chemical shifts, site-dependent shielding tensors in crystalline solids, and adsorption shifts for molecules on surfaces. The Xe chemical shift of xenon gas trapped in the channels and cages of zeolites exhibits large changes with type of zeolite, and for the same zeolite it is found to be extremely dependent on the amount of adsorbed xenon, changing with loading in a way that is unique for each zeolite type so that such behaviour serves as a fingerprint of zeolites. There are no changes in molecular geometry or bonding involved here, merely the effects of neighbouring atoms on the Xe chemical shift, that is, the oxygen atoms of the framework, the counter-ions, and the other Xe atoms that it encounters in the intrazeolitic pores. Even where the average distance between neighbouring atoms is extremely large, as in the dilute gas phase, the NMR chemical shift is found to change with this average distance, exhibiting a dependence on the density and the temperature. This second virial coefficient of shielding can be measured more accurately than the second virial coefficient of any other molecular electronic property. When the chemical shift in a molecule in the gas phase is extrapolated to zero density, one would expect to obtain the chemical shift of an effectively isolated molecule, with no neighbour effects. This too is found to be changing with temperature. Furthermore, when a molecule is observed in the same solution with its deuterated counterpart, a nucleus in the heavier isotopomer is usually more shielded than the same nucleus in the lighter isotopomer. This isotope shift is sometimes observed even when the NMR nucleus and the site of isotopic substitution are separated by several bonds, as many as nine or more bonds, the signs and magnitudes of the isotope shifts changing across the periodic table.

How do we explain these observations? We shall see that these phenomena are due to the dependence of the nuclear shielding on the configuration of the nuclei, the distances between them, the bond angles and

torsion angles between them; in other words, we shall consider the multidimensional shielding surface which describes the variation of the shielding with nuclear positions, analogous to the potential energy multidimensional surface. Not only is the value on this shielding surface at the minimum energy (equilibrium) geometry closely associated with the value that is observed, but the averaging over this surface during the rotation, vibration, and translational motions of the nuclei determines the shielding value that is observed. The observed chemical shift is averaged not only over all the populated rovibrational states, torsions and librations, but also over all the ensembles of the molecule with its neighbours in the gas or solution or adsorbed fluid on a heterogeneous surface. No other molecular electronic property has been characterized so well in terms of the virial coefficients, the mass dependence, and the temperature dependence. The ultra-high resolution afforded by the NMR measurement combined with the exquisite sensitivity of the shielding together make it possible to characterize this molecular property in detail experimentally. The change of the electric dipole polarizability with internuclear separation in a rare gas pair, for example, is one of the "pair interaction properties" that serve very well as tests of theories and physical models but are very difficult to measure. Contrast this with the ^{129}Xe shielding as a function of density and temperature in the dilute gas. Few property surfaces have been explored in their dependence on intramolecular nuclear coordinates. The only electronic property that has a well-known dependence on bond length is the dipole moment, and then only for a diatomic molecule. The experimental observations of the temperature dependence in the rotating-vibrating isolated molecule and the changes upon substitution of a remote atom by a heavier isotope are well characterized in the chemical shift, unlike any other molecular electronic property. The theories associated with the rovibrational averaging of any electronic property can be tested for this property, where both experiments and theoretical calculations are feasible. In other words, the NMR shielding serves as a paradigm for the exploration of the dependence of a molecular electronic property on intramolecular coordinates and masses, as well as intermolecular separations, dependence on the temperature, electric fields and field gradients, and grand ensemble configurations.

In this review we will consider nuclear shielding surfaces in simple systems: diatomic molecules to focus on the variation with bond length, H_2O , NH_3 , PH_3 and CH_4 to consider bond angles and bond lengths, CH_3CH_3 through isobutane to see the dihedral angle dependence and bond angle effects. The variations with ϕ , ψ and χ angles are explored in various model peptides, and finally the remote bond stretches. Following the intramolecular shielding surfaces we move on to intermolecular shielding in atom-atom pairs, atom-ion, and atom-molecule pairs, and clusters of three or more, including up to five or 16 polar solvent molecules. The effects of

electric fields and electric field gradients on shielding are considered separately. Finally we tie these all together in an examination of possible global shapes of the traces on shielding surfaces. Dynamic averages over these surfaces are necessary for comparisons with experiment. Here we show the origin of the temperature dependence, the isotope shifts, the shifts with density and solvent, and hydrogen-bonding shifts. Ensemble averages are sometimes necessary to account properly for the observed cluster shifts and the average chemical shifts under fast exchange in porous media. Finally, we consider the prognosis for more complex systems. What can we say, in general, from the studies on these systems that may shed some light on shielding in more complex systems? How may the methods applicable to small systems be brought to bear on the prediction of chemical shifts in complex materials such as proteins where some electrostatics, some hydrogen bonding, some local bond angle and torsional constraints, and some long-range contributions apply?

2. SHIELDING SURFACES

A shielding surface is a mathematical surface providing the nuclear shielding value (usually the isotropic average over all magnetic field directions, but may also be an individual tensor component) as a function of the nuclear coordinates of the system. In the case of an isolated molecule, the intramolecular shielding surface is usually expressed in terms of nuclear displacement coordinates, such as curvilinear internal coordinates or the symmetry adapted linear combinations of these, the symmetry coordinates. In the case of intermolecular shielding surfaces, the internal coordinates of the supermolecule are used and the shielding is expressed relative to the completely separated interacting molecules including counterpoise corrections. The theoretical shielding surfaces that will be discussed in this review have been calculated using a variety of methods. The conventional Coupled Hartree Fock (CHF) method involves using a common gauge origin in the calculation and generally requires a larger set of basis functions to achieve the gauge independence. This method has been developed by Stevens, Pitzer and Lipscomb,¹ and by Lazzeretti and Zanasi.² At the next level the common origin method is employed in Second Order Polarization Propagation Approach (SOPPA) primarily by Oddershede and coworkers³ and in Coupled MP2 by Bishop and Cybulski,⁴ traditionally using large basis sets to achieve gauge independence. There are several distributed gauge origin approaches: the localized orbital local origin method (LORG) devised by Hansen and Bouman,⁵ and its correlated level called SOLO (Second Order LORG),⁶ the Individual Gauge for Localized Orbitals (IGLO) which has been developed by Schindler and Kutzelnigg,⁷ and its correlated version MC-IGLO by van Wüllen and Kutzelnigg,⁸ and a third method, Gauge-

including Atomic Orbitals (GIAO) originally introduced by Ditchfield,⁹ used extensively by Chesnut, made more efficient by Wolinski, Hinton and Pulay,¹⁰ and rederived especially for correlated calculations by Gauss in MP2-GIAO.¹¹ The review by Chesnut in this volume¹² discusses the recent developments in these *ab initio* methods, and is not a subject of the present review. Our main concern is the resulting shielding surfaces, calculated by one of these methods at some appropriate basis set size. Theoretical calculations of nuclear shielding surfaces for small molecules have been reviewed recently.¹³

2.1. Intramolecular shielding surfaces

2.1.1. Dependence on bond length in diatomic molecules

The first complete shielding surface was calculated for the H_2^+ molecule by Hegstrom.¹⁴ This surface showed the nuclear shielding for the separated atoms, all the way from 22 a.u. to the united atom, which in this case was an He^+ ion. From the large positive united atom value, the shielding is found to decrease until it reaches a minimum which occurs at an internuclear separation much longer than the equilibrium bond length and proceeds to the limiting value at infinite separation. Prior to this complete surface, however, the behaviour of the shielding in diatomic molecules in the immediate vicinity of the equilibrium geometry had already been discovered in the calculations by Stevens and coworkers for LiH ,¹⁵ HF ,¹⁶ CO ,¹⁷ and N_2 .¹⁸ The derivative of the shielding with bond distance was found to be negative in all cases except for the Li nucleus in LiH . Ditchfield's calculations of shieldings in the vicinity of the equilibrium bond length verified these results for LiH and for HF , and in addition provided similar results for the H_2 molecule.¹⁹ Chesnut evaluated first derivatives of the shielding for the first- and second-row hydrides and found similar results for H_2 , HF and HCl : NaH behaved similarly to LiH ²⁰ and the second derivatives in HCl and HF ,²¹ as well as CO , N_2 , CN^- , and F_2 ,²² were also negative for all nuclei. That is, both nuclei in the diatomic molecule become deshielded as the bond lengthens, with the exception of the Li and the Na nuclei in LiH and NaH . The unusual behaviour of the alkali nuclei remained a puzzle until the complete shielding surface of the NaH molecule was calculated by Jameson and de Dios.²³ The complete surface for ^{23}Na in the NaH molecule looks very similar to the shielding surface for the H_2^+ molecule, as shown in Fig. 1. The equilibrium internuclear separation occurs at a bond length shorter than that separation at which the shielding is a minimum in H_2^+ , as it does for the nuclei in diatomic molecules mentioned above and also for ClF .²³ On the other hand, the equilibrium internuclear separation occurs at a distance longer than that for the minimum in the shielding surface of the Na nucleus in the NaH molecule.

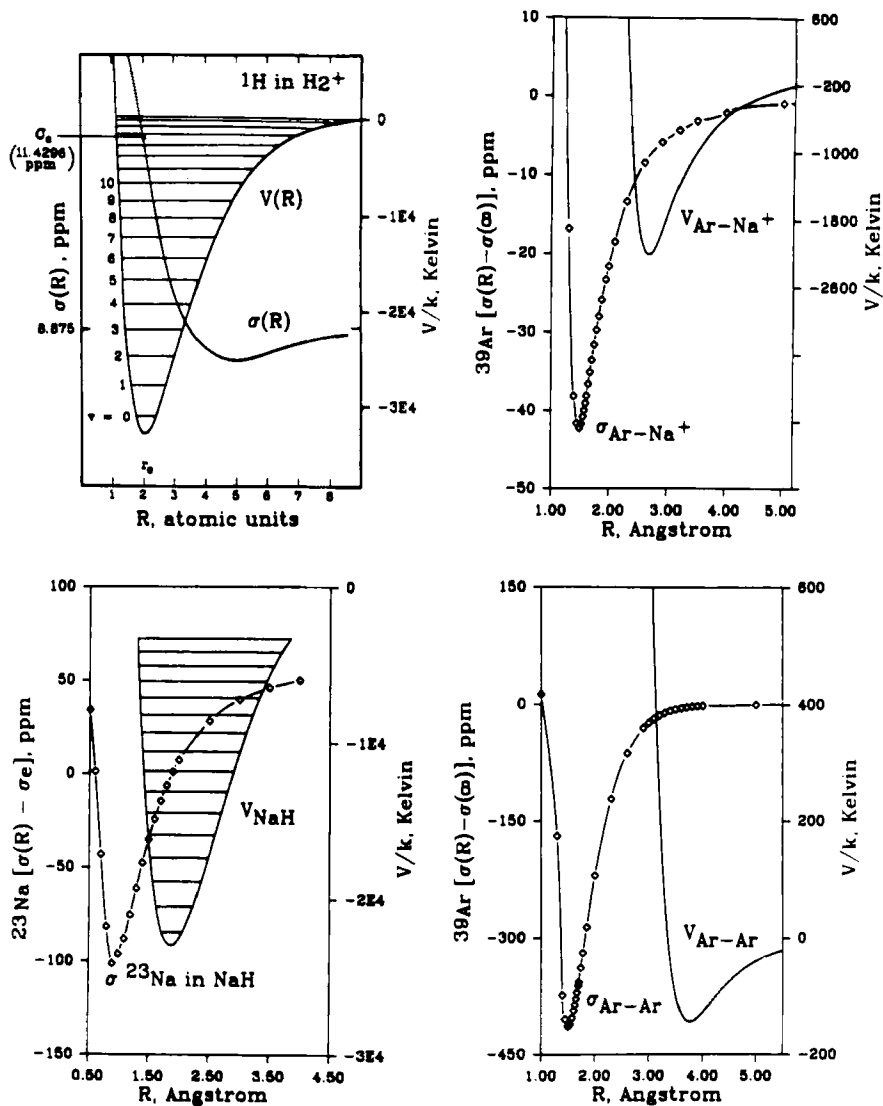


Fig. 1. Nuclear shielding surfaces from *ab initio* calculations. Reproduced from Ref. 23, with permission. The H_2^+ surface is from Hegstrom,¹⁴ the ^{23}Na in NaH surface is from Ref. 23, and the ^{39}Ar in $\text{Ar}-\text{Na}^+$ and $\text{Ar}-\text{Ar}$ intermolecular shielding surfaces are from Ref. 24. The last three were calculated using the LORG method.²⁵ The corresponding potential energy surfaces are from Wind,²⁶ Giroud and Nedelec,²⁷ Viehland,²⁸ and Aziz and Chen,²⁹ respectively.

2.1.2. Bond extension and angle deformation in small molecules

For triatomic and larger polyatomic molecules, the shielding surface is of higher dimension. The surface is best expressed in the nuclear displacement coordinates of the molecule, such as symmetry coordinates. Derivatives evaluated at the equilibrium geometry are, of course, easily converted from one set of coordinates to another. Examination of the details of the shielding surface is best carried out by displaying traces on the surface corresponding to keeping some of the coordinates constant. This was done for the first time by Raynes and coworkers for the nuclei in the H_2O molecule,³⁰ followed by the nuclei in the CH_4 molecule.³¹ Jameson, de Dios and Jameson calculated the shielding surfaces for the N nucleus in NH_3 ³² and P in PH_3 .³³ In these calculations the inversion coordinates of both NH_3 and PH_3 were explored over a wide range of values.^{32,33} When examined together (Fig. 2), these four surfaces have some features in common. The shielding of the non-H nuclei uniformly decreases with an increase in the symmetric stretch coordinate. The asymmetric stretch coordinates and the asymmetric angle deformation coordinates have zero first derivatives by symmetry, and therefore these traces are symmetric functions with respect to positive or negative displacements away from the equilibrium coordinates. They are concave in opposite directions. One (the asymmetric stretch) is concave downward (deshielding with increasing displacement from equilibrium), whereas the other (the asymmetric angle bend) is concave upward (increasing shielding with increasing displacement from equilibrium). A very interesting result is found when the variation of the shielding with respect to the opening of the bond angle is examined in the H_2O , NH_3 , and PH_3 molecules, the bond lengths being kept constant. This trace on the shielding surface is concave upward and has its minimum shielding at the tetrahedral angle.³³ Chesnut had reported some calculations in which the bond lengths are continuously optimized while the bond angle is varied. This is of course a more complicated representation in that both bond length and bond angle are changing at once. Nevertheless, he finds that the shielding surfaces are concave upwards and in H_2S the surface is very flat from 90° to 140° in this representation and for PH_3 his minimum also occurs at the tetrahedral angle.²⁰ The equilibrium angle for H_2O and NH_3 is very close to tetrahedral, whereas for H_2S , H_2Se , and PH_3 it is less than tetrahedral. H_2Se and PH_3 shielding surfaces have a sizeable slope at the equilibrium bond angle.^{33,34}

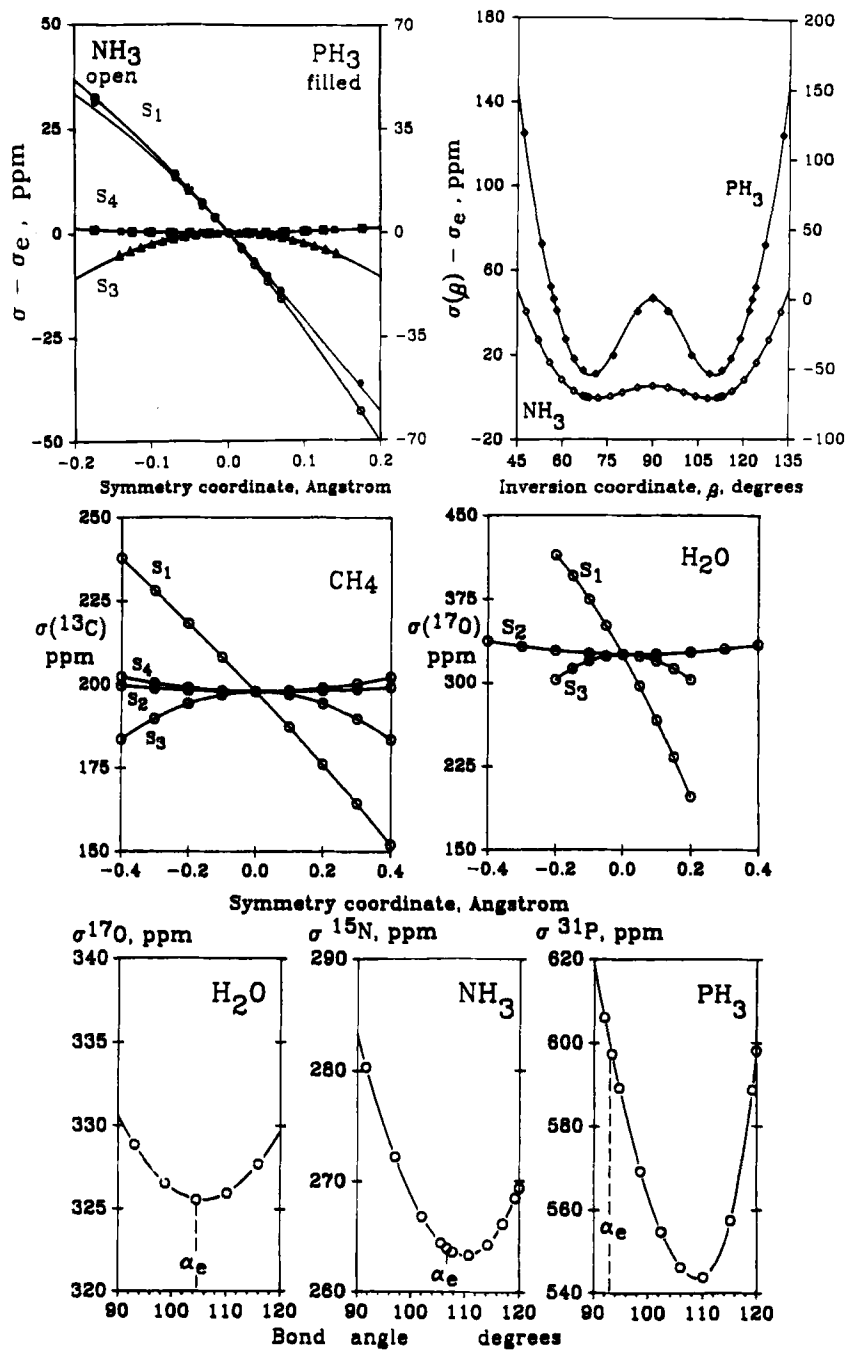
Other molecules have only been studied in terms of the derivatives of the shielding with respect to bond extension at the equilibrium geometry. The first derivatives of the shielding with respect to bond lengthening in the first- and second-row hydrides were calculated by Chesnut.²⁰ Be in BeH_2 , Mg in MgH_2 , B in BH_3 and Al in AlH_3 , all were found to have positive derivatives. The first derivatives of the non-H nuclear shielding in these

hydrides changed smoothly in going from left to right in the Periodic Table, rising to a maximum at group 2 and dropping to large negative values toward group 7. This smooth change has been explained²³ as we shall find in a later section of this review. A comprehensive survey of first and second derivatives of the shielding for molecules containing first-row atoms by Chesnut and Wright³⁵ confirmed earlier predictions. In discussing these we make a distinction of primary (with respect to the stretch of the bond to the nucleus in question) and secondary (with respect to the stretch of a remote bond) derivatives:

- (1) Most of the primary first derivatives are negative, that is, a nucleus tends to become deshielded upon extension of a bond in which it is involved. In this study, only 13 out of about 270 primary first derivatives were found to be positive. Negative derivatives ranged from -4 to $-2784 \text{ ppm } \text{\AA}^{-1}$. The few positive derivatives ranged from $+0.3$ to $+39.0 \text{ ppm } \text{\AA}^{-1}$.
- (2) The derivatives with respect to extension of a multiple bond are generally larger than those involving the extension of a single bond.
- (3) The shielding derivatives with respect to extension of a bond to hydrogen are generally smaller than those involving extension of bonds to heavy atoms.
- (4) The paramagnetic terms dominate the shielding derivatives.
- (5) The shielding derivatives of non-hydrogen nuclei tend to parallel the equilibrium isotropic shielding itself, independent of the nuclear species involved, that is, the shielding derivative decreases algebraically as the isotropic shielding of the nucleus decreases, but especially so for multiple bonds. An example is shown in Fig. 3.

It should be noted that all these general trends had already been proposed much earlier by Jameson³⁶⁻³⁸ and by Jameson and Osten^{39,40} (see Ref. 40 for references) in their interpretation of the very large body of experimental isotope shift data and the temperature dependence of the chemical shifts in the zero-pressure limit of ^{19}F in several molecules and ^{13}C in CO and CO_2 , ^{15}N in N_2 and NNO . Indeed it was the general trends in the experimental data that formed the basis for the interpretation. While the rovibrational averaging theory was complete, the experimental data could not be inverted

Fig. 2. Traces on the shielding surfaces of ^{17}O in the H_2O molecule,³⁰ ^{13}C in CH_4 ,³¹ ^{15}N in NH_3 ,³² and ^{31}P in PH_3 .³³ The symmetry coordinate S_1 is the totally symmetric stretch, S_2 is the symmetric angle deformation or the inversion coordinate (in the case of NH_3 and PH_3). S_3 and S_4 are the asymmetric stretches and angle deformations, respectively.



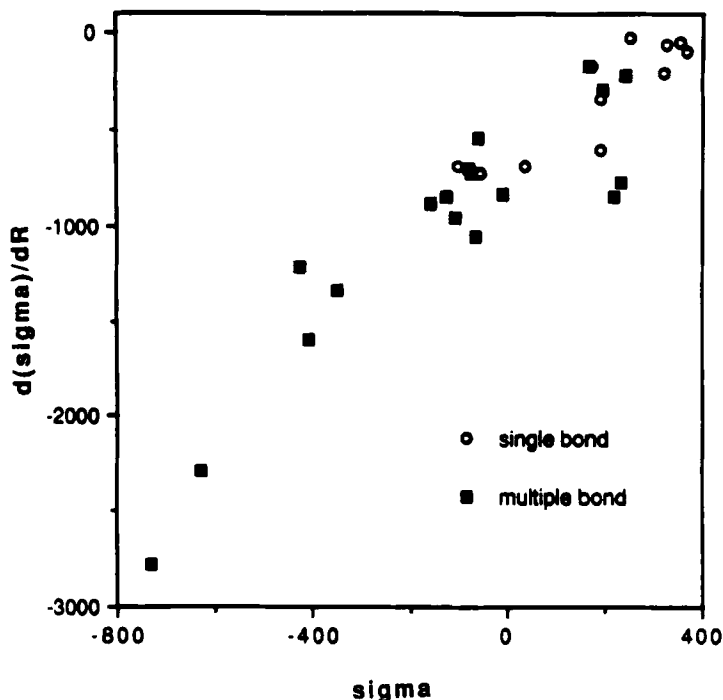


Fig. 3. The first derivatives of the ^{17}O shielding with respect to extension of the bond correlates with the absolute shielding. Reproduced from Ref. 35 with permission of John Wiley & Sons, Inc. Copyright © 1991 John Wiley & Sons, Inc. These are *ab initio* values calculated using the GIAO method.

to provide more than the empirical derivatives $(\partial\sigma^X/\partial r_{AX})_{\text{eq}}$. The ability of local origin methods to describe adequately the shielding even with modest basis sets has now made possible the theoretical investigations of these earlier conclusions and to find their limitations and conditions of applicability.³⁵ Furthermore, Chesnut's survey of shielding derivatives offers new information about second derivatives $(\partial^2\sigma^X/\partial r_{AX}^2)_{\text{eq}}$. Most of the second derivatives are negative, that is, a nucleus tends to become deshielded upon bond extension in a more pronounced way than linearly. Of the 210 second derivatives, 42 were found to be positive (these involved proton shieldings in most cases). Second derivatives are not small, that is, the trace along the shielding surface corresponding to a symmetric stretch of the bonds is not linear at the point corresponding to the equilibrium geometry of the molecule.

The shielding dependence on bond length has also been examined in model fragments (*N*-formyl-L-amino acid amide) for glycine, alanine and valine residues in proteins.⁴¹ Likewise, in these model compounds, the first

and second derivatives of the C^α chemical shielding with respect to its bond lengths, $C^\alpha-N$, $C^\alpha-C^O$, $C^\alpha-H^\alpha$ and $C^\alpha-C^\beta$ (for alanine and valine) are found to be negative. The magnitudes of these derivatives were sufficiently large (40–90 ppm \AA^{-1}) to permit an evaluation of the spread of bond length values for a particular residue reported in X-ray structures of proteins.⁴² After considering the range of chemical shift inequivalencies observed in proteins, it has been deduced that the differences in bond lengths currently reported in X-ray structures are too large to be consistent with NMR data.

An interesting observation that can be made from these studies is the apparent transferability of these shielding derivatives from one amino acid to another. Both alanine and valine have very similar first derivatives for the shielding of C^α with respect to the $C^\alpha-N$ stretch (Ala; $-88 \text{ ppm } \text{\AA}^{-1}$, Val; $-84 \text{ ppm } \text{\AA}^{-1}$), $C^\alpha-C^O$ (Ala; $-57 \text{ ppm } \text{\AA}^{-1}$, Val; $-60 \text{ ppm } \text{\AA}^{-1}$), and $C^\alpha-C^\beta$ (Ala; $-16 \text{ ppm } \text{\AA}^{-1}$, Val; $-17 \text{ ppm } \text{\AA}^{-1}$). On the other hand, even though glycine lacks C^β , its derivatives are not too far from alanine and valine: $C^\alpha-N$ ($-69 \text{ ppm } \text{\AA}^{-1}$) and $C^\alpha-C^O$ ($-48 \text{ ppm } \text{\AA}^{-1}$). The glycine derivatives being numerically 80% of the alanine and valine derivatives may reflect in the ground-state vibrational corrections as pointed out by Laws *et al.*⁴²

The corresponding C^β shielding derivatives also show some interesting characteristics. First of all, the first derivatives of C^β shielding with respect to the bond lengths $C^\alpha-N$ and $C^\alpha-C^O$ were found to be positive in sign.⁴¹ On the other hand, its derivative with respect to $C^\alpha-H^\alpha$ is still negative but an order of magnitude smaller ($-7 \text{ ppm } \text{\AA}^{-1}$ for C^β compared to $-57 \text{ ppm } \text{\AA}^{-1}$ for C^α). The dependence of the C^β shielding on the bond length $C^\alpha-C^\beta$ appears to be normal. It is noteworthy, however, that the two model fragments, alanine and valine, differ greatly in magnitude in terms of this shielding derivative. Alanine has $-36 \text{ ppm } \text{\AA}^{-1}$ for $\partial\sigma^{C^\beta}/\partial r(C^\alpha-C^\beta)$ while valine has $-69 \text{ ppm } \text{\AA}^{-1}$, nearly twice the value for alanine. This difference indicates that the presence of methyl groups on C^β in valine leads to a greater sensitivity of the C^β shielding to the $C^\alpha-C^\beta$ bond length. This is consistent with the well-known incremental effects of methyl substitution in deuterium-induced isotope shifts.

The dependence of shielding on bond angle as seen in small molecules is much more complicated than its dependence on bond length. In fact, using the first derivative of the shielding with respect to bond length normally would suffice. On the other hand, the shielding as a function of bond angle in Fig. 2 shows definite curvature. And as observed in the small hydrides (Fig. 2), an extremum (minimum shielding) is found near the tetrahedral value. Hence, in order to take into account bond angle influences on shielding, one needs to take into account higher-order derivatives. The same trends are seen in model fragments for amino acid residues in proteins. Glycine, for example, shows a minimum for the C^α shielding when the $N-C^\alpha-C^O$ angle is close to the tetrahedral value,⁴¹ the surprising feature